Available online at www.sciencedirect.com
SCIENCE DIRECT®
International Journal of Mass Spectrometry 235 (2004) 171–178
International Journal of Mass Spectrometry
www.elsevier.com/locate/ijms

Resonance ionization mass spectrometry for ultratrace analysis of plutonium with a new solid state laser system

C. Grüning [a], G. Huber [b], P. Klopp [a], J.V. Kratz [a], P. Kunz [b], G. Passler [b], N. Trautmann [a,*], A. Waldek [a], K. Wendt [b]

[a] *Institut für Kernchemie, Universität Mainz, D-55099 Mainz, Germany*
[b] *Institut für Physik, Universität Mainz, D-55099 Mainz, Germany*

Received 1 March 2004; accepted 29 April 2004

Available online 8 June 2004

Abstract

Resonance ionization mass spectrometry (RIMS) is well-suited for isotope selective ultratrace analysis of long-lived radioactive isotopes due to its high element and isotope selectivity and good sensitivity. For the analysis of plutonium with a pulsed RIMS apparatus, a powerful, reliable and easy to handle Nd:YAG pumped titanium–sapphire laser system has been developed and combined with a time-of-flight mass spectrometer. Spectroscopic measurements led to an efficient three step excitation and ionization scheme for plutonium with $\lambda_1 = 420.76$ nm, $\lambda_2 = 847.28$ nm, and $\lambda_3 = 767.53$ nm. The isotope shifts in this scheme for the plutonium isotopes ^{238}Pu through ^{244}Pu have been determined. An overall efficiency of the RIMS apparatus of 1×10^{-5} is routinely achieved resulting in a detection limit of 2×10^6 atoms of plutonium for single isotope measurements. The application of RIMS for isotope ratio measurements is outlined.

Keywords: Titanium–sapphire laser; Resonance ionization mass spectrometry; Ultratrace detection; Plutonium

1. Introduction

Trace amounts of plutonium were and are still released into the environment as a result of nuclear weapons tests, accidents, and releases from nuclear facilities. The isotopic composition of a plutonium contamination is directly related to its origin through the production method and its parameters [1,2]. Plutonium as a by-product from nuclear power plants can be used for nuclear weapons, as fuel for power plants, or treated as waste. Therefore, a fast, sensitive and isotope selective detection method for plutonium is required for nuclear safeguards and forensics, personnel dose monitoring, risk assessments in case of nuclear accidents, studies of the migration behavior in the context of long time storage of nuclear waste, and low-level surveillance of the environment.

Alpha-spectroscopy as the standard method of plutonium detection is not well-suited for the isotope selective determination. The detection limit and the measuring time depend on the half-life of the isotope under investigation, yielding a detection limit of, e.g., 4×10^8 atoms for ^{239}Pu in 1000 min counting time [3]. Furthermore, with this technique, it is rather difficult to distinguish between ^{239}Pu and ^{240}Pu due to their very similar α-energies (^{239}Pu: 5.157 MeV, ^{240}Pu: 5.168 MeV), and ^{241}Pu as a β-emitter cannot be detected at all. Conventional mass spectrometric detection methods like TIMS [4] or ICP-MS [5–8] are independent of the decay type and half-life of the isotope, but their ionization process is quite unspecific with respect to different elements or molecules leading to possible isobaric interferences. In the case of plutonium, these are caused mostly by ^{238}U, which is always present in large excess in environmental samples, or by ^{241}Am, a decay product of ^{241}Pu. The use of hyphenated techniques as one possibility to avoid these isobaric interferences, i.e., the separation of different elements with the help of chemical procedures like chromatographic separations or capillary electrophoresis prior to the detection with mass spectrometry, make these methods more complex. With multiple collector sector field ICP-MS systems, plutonium contents and isotope ratios have been recently

* Corresponding author. Tel.: +49 6131 39 25847; fax: +49 6131 39 24488.
E-mail address: norbert.trautmann@uni-mainz.de (N. Trautmann).

1387-3806/$ – see front matter © 2004 Elsevier B.V. All rights reserved.
doi:10.1016/j.ijms.2004.04.013

measured directly at ultratrace levels down to 10^7–10^8 atoms [9–12]. Accelerator mass spectrometry (AMS), which provides extremely high isotopic selectivities up to 10^{15} and detection limits down to 10^4 atoms [13] has also been applied to plutonium recently [14,15]. However, a drawback of this technique is its high experimental expenditure.

With its element and isotope selective ionization process, resonance ionization mass spectrometry (RIMS) has been developed and applied starting more than a quarter century ago [16] as an excellent method for the isotope selective ultratrace analysis of plutonium as well as for other elements [17,18]. Using a copper vapor laser pumped dye laser system, RIMS has been applied for ultratrace analysis of plutonium and other radioactive isotopes [19–21] and for spectroscopic investigations of actinides [22,23]. As the copper vapor laser based system requires very high maintenance efforts and is very costly it is not suitable for routine measurements. Therefore, a new solid state laser system has been set up that is described in this paper together with its use for spectroscopic investigations of plutonium in order to make the application of RIMS easier for the isotope specific analysis of plutonium as compared to the copper vapor laser based system.

2. Resonance ionization mass spectrometry (RIMS)

For ultratrace analysis of plutonium by RIMS, three steps are required. In the first step plutonium is separated chemically using a simple procedure and the isolated fraction is thermally evaporated from an atomic beam source into vacuum. Then, starting from the ground state or a low lying excited state of atomic plutonium, multi-step resonant excitation is performed by means of laser light in order to populate high-lying states with subsequent ionization. This process results in an excellent elemental selectivity. Thus, isobaric interferences are completely suppressed during the ionization process. Isotope selectivity is provided in our setup by mass analysis of the ions in a mass spectrometer, which also serves for efficient background suppression. Additional isotope selectivity, if necessary, can be achieved in the resonance and ionization process through the use of lasers with narrow bandwidth, exploiting the isotope shifts in the optical transitions [24,18].

For plutonium with its ionization potential of 6.0261(1) eV [25], an excitation and ionization scheme starting from the electronic ground state and using three photons provides sufficient elemental selectivity. The probability of accidentially matching a transition of an unwanted atomic species like uranium, e.g., is found to be negligible, if the level density in atoms and the laser bandwith is compared [8]. As the isotopic selectivity needs to be only moderately high, a RIMS system with pulsed lasers of moderate spectral bandwidth has been set up. This enables the use of a time-of-flight mass spectrometer (TOF-MS) where the laser pulse delivers the start signal and the incoming photoion the stop signal. This has the advantage of detecting all isotopes simultaneously.

3. Experimental setup

The complete RIMS setup is shown in Fig. 1. The laser light for the resonant excitation of plutonium is generated with the new Nd:YAG pumped titanium–sapphire (Ti:Sa) laser system described in more detail in the next section. In order to ionize plutonium in three steps with laser light available from three Ti:Sa lasers, the light for the first excitation step is frequency doubled by means of a β-barium-borate crystal. The three laser beams are sent through a $\varnothing = 200\,\mu m$ multimode optical fiber to ensure a good spatial overlap and are transported to the ionization region of the time-of-flight mass spectrometer with a transmission of approximately 60%.

For an efficient ionization of plutonium in the source region of the TOF-MS, a sandwich filament with tantalum as backing material onto which $Pu(OH)_4$ is electrolytically deposited and covered with a ~1 μm thick sputtered layer of titanium as a reducing agent is used [26]. This filament is resistively heated from 1150 to 1400 K.

Under these conditions, $Pu(OH)_4$ is converted to plutonium oxide, which diffuses through the titanium layer. During the diffusion process, it is reduced to Pu and evaporates from the titanium surface. With this filament type the evaporation of plutonium occurs at relatively low

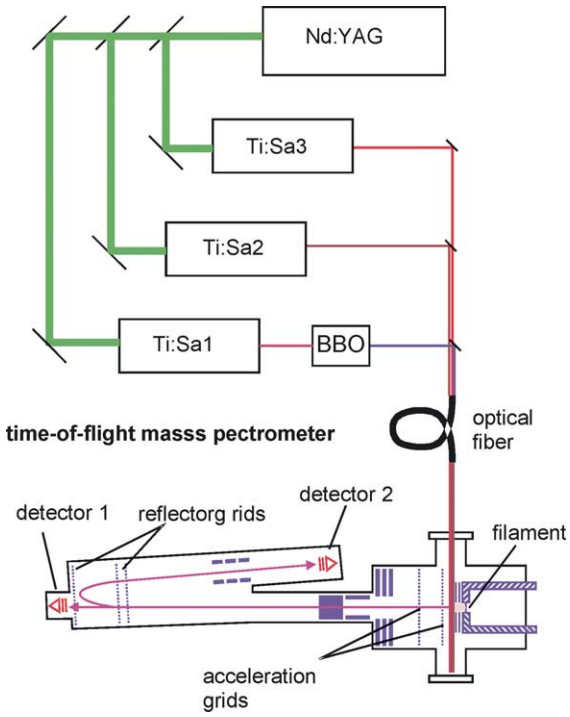

Fig. 1. Setup of the pulsed RIMS system with a Nd:YAG pump laser, three titanium–sapphire lasers, and a TOF-MS.

temperatures and therefore thermal ionization is avoided. According to the Boltzmann distribution, about 80% of the plutonium atoms remain in the ground state at the evaporation temperature. Within a measuring time of typically 1 h, the temperature is slowly increased from 1150 to 1400 K to compensate for depletion until the plutonium is completely evaporated. The atoms are resonantly ionized as they cross the laser beams, subsequently mass separated in the TOF mass spectrometer with a resolution of $m/\Delta m_{\mathrm{FWHM}} \approx 600$ and finally registered by multi-channel plate detectors. The setup of the reflectron mass spectrometer as well as the data acquisition system have already been described [20,27]. For all experiments described in the following, the TOF-MS has been operated in the reflectron mode and the vacuum system had a background pressure of about 10^{-6} Torr. Since the copper vapor laser pumped dye system was not suitable for the routine trace analysis of plutonium and other actinides a new laser system was developed with the following specifications:

- High repetition rate to obtain a good duty cycle in combination with the filament technique that evaporates atoms continuously.
- High output power to saturate the optical transitions, resulting in a high excitation/ionization efficiency.
- Laser line widths of the same order of magnitude as the width of the Doppler-broadened optical transitions of the excitation scheme for plutonium in order to use the whole spectral intensity for the excitation.
- Lower maintenance and easier to handle.

4. Solid state laser system

As pump laser, a commercially available intra cavity frequency doubled Nd:YAG laser (Clark-MXR ORC-1000) is used. This laser operates at a wavelength of 532 nm and delivers an average laser power of up to 50 W at a repetition rate in the 5–10 kHz range. Its relatively long pulse duration of more than 200 ns prevents its use for pumping dye lasers because of the much shorter fluorescence lifetimes of the excited states of laser dyes. As an alternative medium to be pumped by this Nd:YAG laser, titanium–sapphire (Ti:Sa) with a fluorescence lifetime of 3.2 μs is well-suited for tunable laser operation. Its broad fluorescence spectrum enables laser operation in a wavelength range from 680 to 1100 nm and its high damage threshold makes it suitable for pulsed systems with high pulse intensities [28]. The pump laser beam with a power of 50 W is split into three beams of approximately the same power by means of two dielectric beam splitters of 33 and 50%, respectively, and guided to the Ti:Sa lasers. The mechanical setup of the Ti:Sa laser is shown in Fig. 2. The beam of the pump laser is focused into the Ti:Sa crystal to ensure a good overlap of the pumping beam with the resonator mode. The crystal, cut in the Brewster angle, is placed in the middle of a 'Z' shaped resonator between two concave mirrors to compensate for

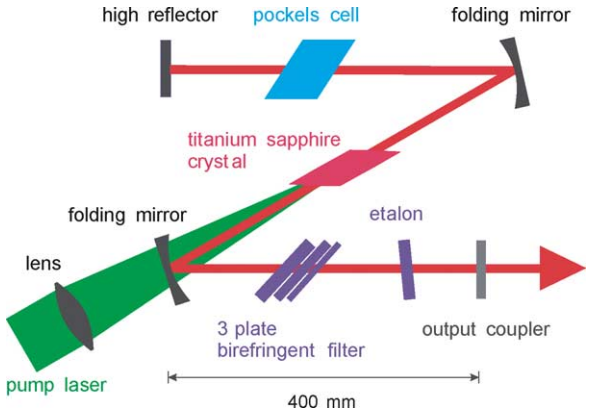

Fig. 2. Mechanical setup of the titanium–sapphire lasers with the 'Z' shaped resonator.

the astigmatism of the crystal [29]. A detailed discussion of this type of resonator layout and the elements for spectral and temporal control will be presented elsewhere [30]. The lasing threshold for this configuration with all optical elements in function has been measured at $\lambda = 767.53$ nm to be $E_{\mathrm{lt}} = 0.26(2)$ mJ per pump laser pulse. With a slope efficiency of $\mathrm{d}E_{\mathrm{Ti:Sa}}/\mathrm{d}E_{\mathrm{pump}} = 0.20(1)$, the laser delivers an average power of about 1.5 W when pumped with 9 W at a repetition rate of 6.6 kHz (see Fig. 3).

For coarse wavelength selection, a three plate birefringent filter with a plate thickness ratio of 1:4:16 (coherent) is used, resulting in a laser line width of approximately $\delta\nu_{\mathrm{FWHM}} = 200$ GHz. In combination with the set of dielectrically coated mirrors, the operating wavelength can be tuned between 740 and 880 nm by turning the birefringent filter (see Fig. 4) [31].

In a 30 nm wide range around $\lambda = 820$ nm, the laser efficiency is somewhat reduced and the laser tends to start on a second lasing mode at a 45 nm shorter wavelength. This behavior can be explained with an interplay of the fluorescence spectrum of the titanium–sapphire crystal, the reflection spectrum of the mirror set and the birefringent filter. In this region, the selectivity of the birefringent filter is not sufficient to suppress the lasing of the second mode efficiently and, therefore, the unwanted wavelength can be present as well. This behavior can be avoided by slightly changing the alignment of the optical components at the cost of reducing the laser efficiency.

A 300 GHz etalon with a reflectivity of $R = 65\%$ placed in front of the output coupler further reduces the laser line width to $\delta\nu_{\mathrm{FWHM}} = 2$–3 GHz, which is of the same order of magnitude as the Doppler widths of the optical transitions of plutonium. The etalon allows scanning of the wavelength continuously over 300 GHz by simply tilting the etalon mount (see insert of Fig. 4). For small wavelength changes of the order of 100 GHz, the output power is stable within 10%. The wavelength selective elements are rigidly mounted and motorized, thus allowing the computer controlled precise selection of the desired wavelength that is mandatory for exact isotope ratio measurements. Wavelength measurements

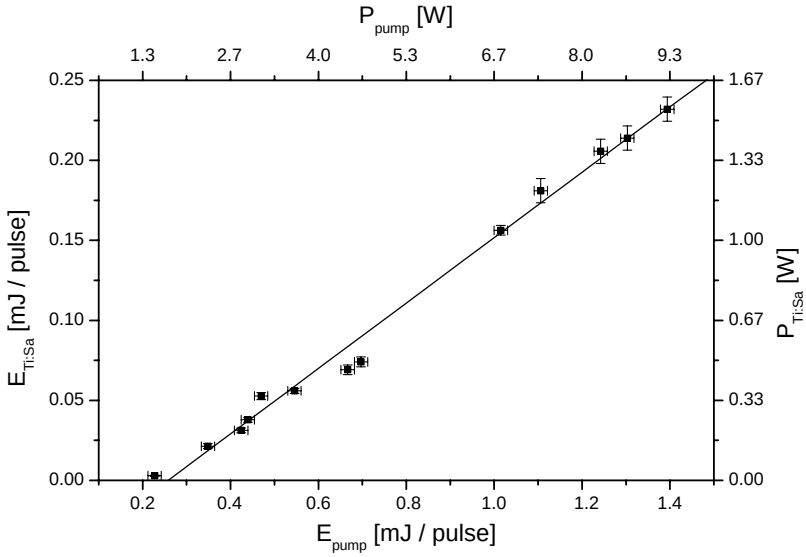

Fig. 3. Energy of the Ti:Sa laser pulse as a function of the pump pulse energy at a wavelength of $\lambda = 767.53$ nm. Average power scales (top and right) refer to 6.6 kHz repetition rate.

have been performed with a Wavemeter LM007 (ATOS) that features a high precision of up to $\Delta\lambda/\lambda = 10^{-7}$ both for pulsed and continuous wave lasers.

The Ti:Sa lasers have a pulse duration of $\Delta T_{\mathrm{FWHM}} = 70$ ns when pumped with an energy of at least 1 mJ per pulse. In order to synchronize the three lasers in time, a pockels cell (BPZ 8, LINOS) is used as a fast Q-switch for the resonator of each laser. The lasers are switched on with a pulse rise time of approximately 10 ns by means of a fast high voltage switch (HTS 51/04, Behlke) that applies 4 kV to the pockels cell. This allows to delay the Ti:Sa laser pulses individually for up to 4 μs relative to the pump pulse. The loss within the first 200 ns, necessary to synchronize the three lasers, lies below 5% and is negligible.

If not stated differently for all measurements described in the following, the laser system was operated with a repetition rate of 6.6 kHz, a pulse width of $\Delta T_{\mathrm{FWHM}} \approx 70$ ns, a beam diameter $d_{\mathrm{FWHM}} \approx 3$ mm, and laser powers with maximum values of $P_{1\mathrm{max}} = 100$ mW, $P_{2\mathrm{max}} = 700$ mW, and $P_{3\mathrm{max}} = 900$ mW, measured at the excitation region of the mass spectrometer.

5. Spectroscopic investigations on plutonium

The isotope selective ultratrace analysis of plutonium by RIMS requires an efficient excitation and ionization scheme. Furthermore, the precise transition wavelengths for

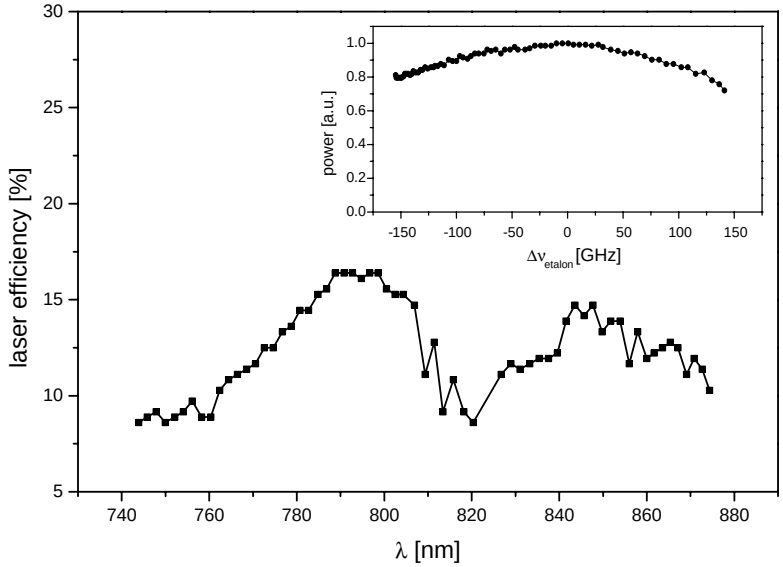

Fig. 4. Tuning range and lasing efficiency of a Ti:Sa laser with a birefringent filter. The insert shows the scanning range of an etalon additionally placed in the Ti:Sa laser with a fixed position of the birefringent filter.

all isotopes of interest as well as the saturation behavior of each excitation step have to be determined. The wavelengths of the excitation scheme with $\lambda_1 = 586.492$ nm, $\lambda_2 = 665.568$ nm, and $\lambda_3 = 577.279$ nm used with the copper vapor/dye laser system [23] lie outside the tuning range of the Ti:Sa lasers, and therefore, a new excitation and ionization scheme had to be exploited [31]. Starting from the plutonium ground state $5f^6\ 7s^2\ ^7F_0$, $J = 0$, frequency doubled Ti:Sa laser light with $\lambda_1 = 420.76\,\text{nm} \equiv 23{,}766\,\text{cm}^{-1}$ populates the state $5f^6\ 7s\ 7p\ ^7D_1$, $J = 1$ and subsequently, light with a wavelength of $\lambda_2 = 847.28\,\text{nm} \equiv 11{,}803\,\text{cm}^{-1}$ leads to a state with $J = 2$. From there, a high lying Rydberg state is populated with $\lambda_3 = 767.53\,\text{nm} \equiv 13{,}029\,\text{cm}^{-1}$. This state is only $7\,\text{cm}^{-1}$ below the first ionization potential of plutonium of IP $= 6.0261(1)\,\text{eV} \equiv 48{,}604(1)\,\text{cm}^{-1}$ and therefore, an electric field with a strength of approximately $1.3\,\text{V cm}^{-1}$ is sufficient for the field ionization of the highly excited plutonium.

In order to perform precise isotope ratio measurements, the exact transition wavelengths of this excitation scheme have been determined for all plutonium isotopes that are of interest, i.e., ^{238}Pu to ^{242}Pu and ^{244}Pu (see Table 1). The scans over all three excitation steps for ^{244}Pu are shown in Fig. 5 applying relatively low laser powers ($P_1 = 1$ mW, $P_2 = 17$ mW, and $P_3 = 600$ mW) to avoid saturation effects. For the first and second step, fits of Gaussian curves with line widths of $\delta\nu_1 = 5.3(1)$ GHz and $\delta\nu_2 = 3.7(1)$ GHz describe the data points quite well. The main contribution to the line widths stems from the laser line width of approximately 3 GHz. Because the laser wavelength is frequency doubled for the first excitation step, its line width is a factor of $\sqrt{2}$ larger and thus, results in $\delta\nu_1 = 5.3$ GHz. For the third step, the transition is best described with a Lorentzian function with a line width of $\delta\nu_3 = 17.4(3)$ GHz.

The level energies and isotope shifts of these levels for those isotopes that were published in the literature, $E_1 = 23{,}766.139(5)\,\text{cm}^{-1}$ and $E_2 = 35{,}568.75(2)\,\text{cm}^{-1}$ for ^{240}Pu and the ^{239,240}Pu isotope shifts of $\text{IS}_1 = 0.155\,\text{cm}^{-1}$ and $\text{IS}_2 = 0.090\,\text{cm}^{-1}$ [32] agree very well with the measured values of $E_1 = 23{,}766.16(2)\,\text{cm}^{-1}$, $E_2 = 35{,}568.75(3)\,\text{cm}^{-1}$, $\text{IS}_1 = 0.16(3)\,\text{cm}^{-1}$ and $\text{IS}_2 = 0.09(3)\,\text{cm}^{-1}$. The isotope shifts in the first and second excitation steps imply that, for correct isotope ratio measurements, the wavelengths of the first and second lasers must be tuned to the exact transition wavelengths of the isotopes of interest whereas for the third step, the wavelength can be fixed at 767.53 nm.

Table 1
Measured transition wavelengths for the plutonium isotopes ^{238}Pu–^{244}Pu

Isotope	λ_1 (cm^{-1})	λ_2 (cm^{-1})	λ_3 (cm^{-1})
^{238}Pu	23,766.40(2)	11,802.45(2)	13,028.80(2)
^{239}Pu	23,766.32(2)	11,802.52(2)	13,028.80(2)
^{240}Pu	23,766.16(2)	11,802.59(2)	13,028.81(2)
^{241}Pu	23,766.11(4)	11,802.64(4)	13,028.79(4)
^{242}Pu	23,765.98(2)	11,802.72(2)	13,028.81(2)
^{244}Pu	23,765.75(2)	11,802.84(2)	13,028.81(2)

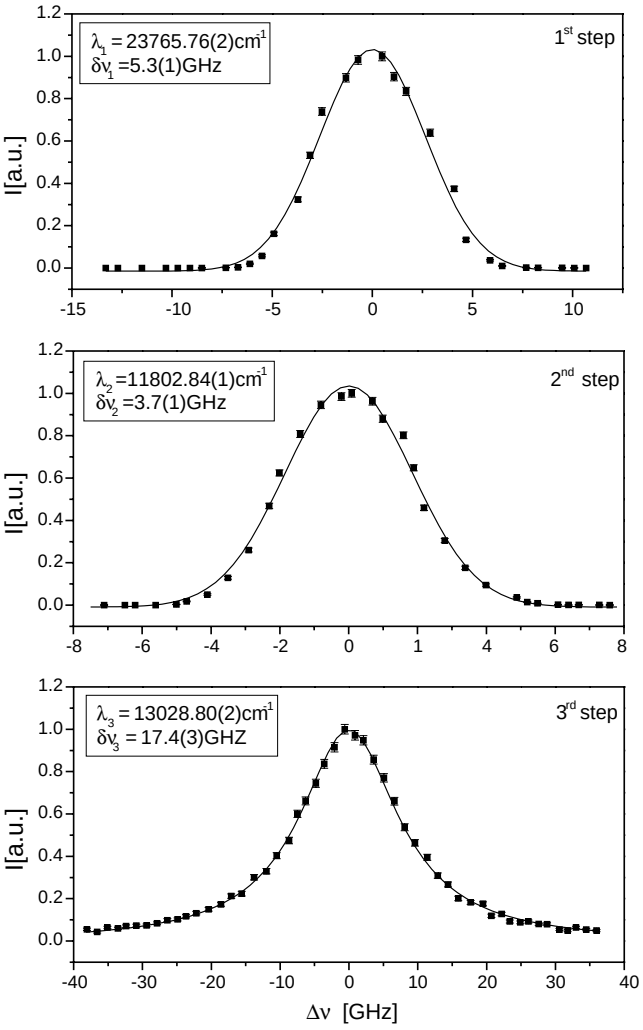

Fig. 5. Laser scan over the resonance frequencies of ^{244}Pu. Gaussian fits for the first and second, Lorentzian fit for the third step.

The knowledge of the saturation behavior of the three excitation steps is of importance, in order to estimate the influence of changes of the laser power on the ionization efficiency during analytical measurements. For this, laser powers were set to the maximum values of $P_{1\text{max}} = 100$ mW, $P_{2\text{max}} = 700$ mW, and $P_{3\text{max}} = 900$ mW. The laser power for the respective excitation step was varied using neutral gray filters. The count rate of plutonium was measured before, during, and after the attenuation of the laser power to account for possible variations in the evaporation rate of plutonium from the filament. An exponential function $I(P) = I_0(1 - e^{-P/P_S})$ that describes in a good approximation the dependence of the transition rates on the laser powers [19] is fitted to the measured values and the plots for ^{240}Pu are shown in Fig. 6. In the first excitation step, the saturation power is $P_{S1} \approx 2$ mW, in the second $P_{S2} \approx 30$ mW, and for the third step, $P_{S3} \approx 400$ mW are

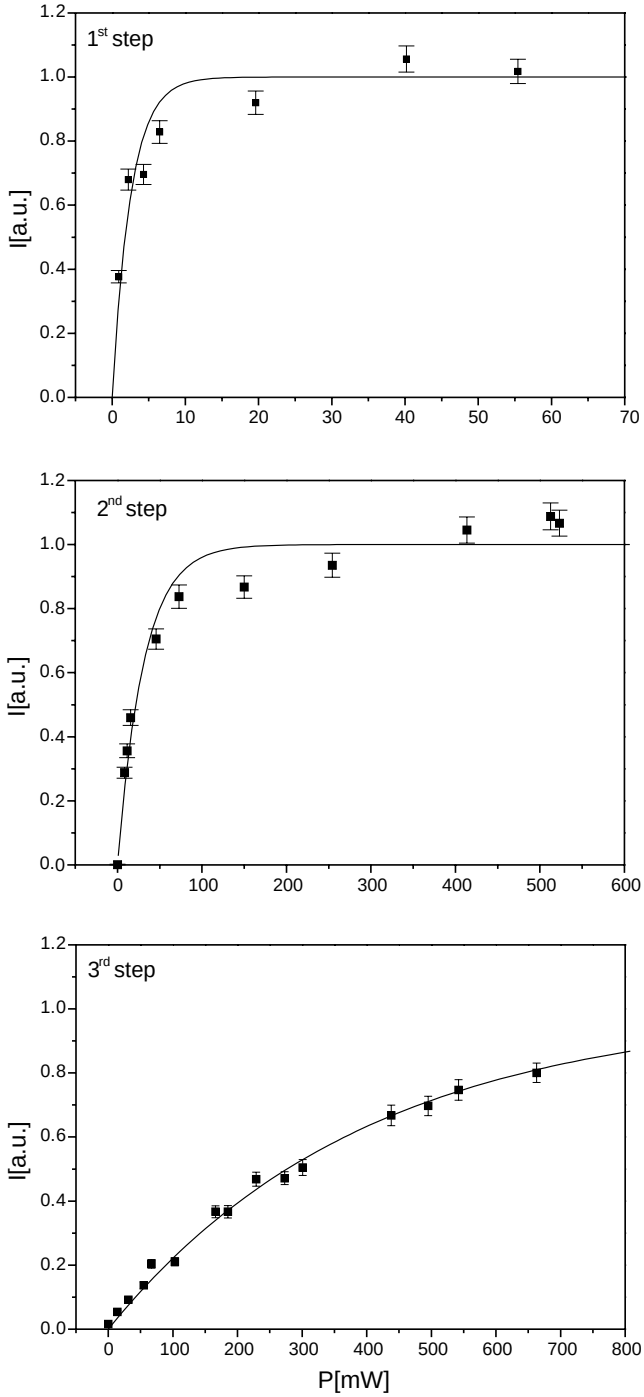

Fig. 6. Saturation behavior of the three excitation steps of plutonium-240. The normalized count rate is plotted vs. the laser power.

necessary. If these powers are compared to the maximum values P_{max} that are available from the lasers and were used during analytical measurements, it is obvious that small drifts in the laser powers result in a change of the ionization efficiency of a few percent only and are therefore negligible.

Another positive effect of high laser powers is the power broadening of the transition lines as shown for the first excitation step of ^{240}Pu in Fig. 7 with a laser power of $P_1 = 95$ mW. The dotted line represents the best Gaussian curve fit to all data points. It is not in accordance with the measured values, and its width of $\delta\nu_G = 9.3(4)$ GHz is much larger than the one measured with $P_1 = 1$ mW, which is shown in Fig. 5. Especially at the center, the measured curve is too flat compared to a Gaussian profile. This is due to the power broadening of the transition. As an important result, the ionization efficiency is quite insensitive to small drifts of the laser wavelengths of a few gigahertz, which avoids the necessity of a very accurate stabilization of the frequency of the Ti:Sa lasers.

6. Characterization of the RIMS setup for ultratrace analysis of plutonium

The RIMS setup with the Nd:YAG pumped Ti:Sa laser system and the excitation and ionization scheme described above has been used for isotope selective ultratrace analysis of plutonium. First, the overall efficiency of the system has been determined in a series of measurements. Filaments with 10^{10} atoms = 33 mBq of ^{240}Pu were prepared and the plutonium content on the filament was determined via α-spectroscopy prior to the RIMS measurement. During the RIMS measurements of about 1 h each, the laser wavelengths were fixed at the corresponding wavelengths for ^{240}Pu with maximum laser powers and all ions on mass 240 were registered to determine the overall efficiency of the setup. This RIMS efficiency is defined as $\varepsilon_{RIMS} = N/F$ with N, number of ions counted at a specific mass and F, number of corresponding atoms deposited on the filament. As illustrated in Table 2, the efficiency varies only slightly around $\varepsilon_{RIMS} = 1 \times 10^{-5}$. Taking into account the very low background count rate, this results in a detection limit of 2×10^6 atoms of plutonium for a single isotope with a 3σ confidence level. This RIMS efficiency is independent of the isotope under investigation, and for the most important environmental isotope, ^{239}Pu, the detection limit is about a factor of 100 lower than that of α-spectroscopy [3].

For the measurements of environmental samples, a known amount of a plutonium tracer isotope, ^{244}Pu, is added prior to the chemical separation to account for variations in the RIMS efficiency as well as in the yield of the chemical isolation. In this way, only isotope ratios and no absolute values must be measured to determine the plutonium content. In order to verify the capability of RIMS to measure isotope ratios, the content of a certified standard has been determined. In Fig. 8, the mass spectrum of a sample containing approximately 10^{12} atoms of ^{244}Pu from the National Institute for Standards and Technology (NIST)—SRM996 plutonium reference material—is shown. During the measurement laser one and two were alternately set for each isotope to the appropriate transition wavelengths from ^{238}Pu to ^{244}Pu. All plutonium isotopes present with mass numbers from 238 to 244 could be detected over a dynamic range of four orders of magnitude. The measured ratios relative to

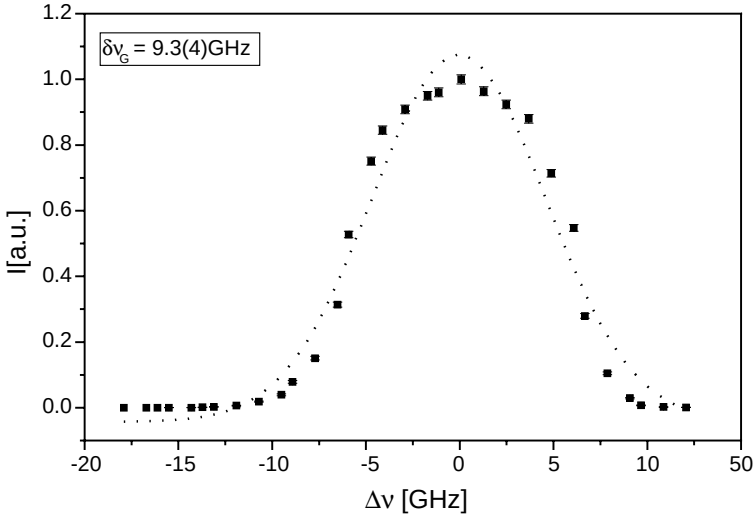

Fig. 7. Laser scan over the first excitation step of ^{240}Pu with $P_1 = 95$ mW. The dotted line represents the best Gaussian fit to all data points.

Table 2
Overall efficiency and detection limit of the RIMS setup for ^{240}Pu taking into account 3σ errors from counting statistics

	Numbers							
	1	2	3	4	5	6	7	8
ε_{RIMS} (10^{-5})	1.6(1)	1.0(1)	2.1(1)	1.3(1)	1.0(1)	0.9(1)	1.2(1)	2.4(1)
DL (10^5 atoms)	13	25	7	4	9	12	8	6

^{244}Pu are presented in Table 3 and agree very well with the certified values.

A slight deviation towards a higher value is observed for the odd-A isotope ^{241}Pu. A somewhat higher RIS efficiency for odd-A isotopes has been reported for other elements and was assigned to the hfs-structure and effects due to angular momenta of different hfs-components covered by the broad-band lasers [33,34]. This effect might be the reason for the overestimation of ^{241}Pu in this measurement as well.

The reliability of the RIMS method was demonstrated with a cocktail containing 10^{10} atoms of ^{244}Pu together with known amounts of the most abundant plutonium isotopes

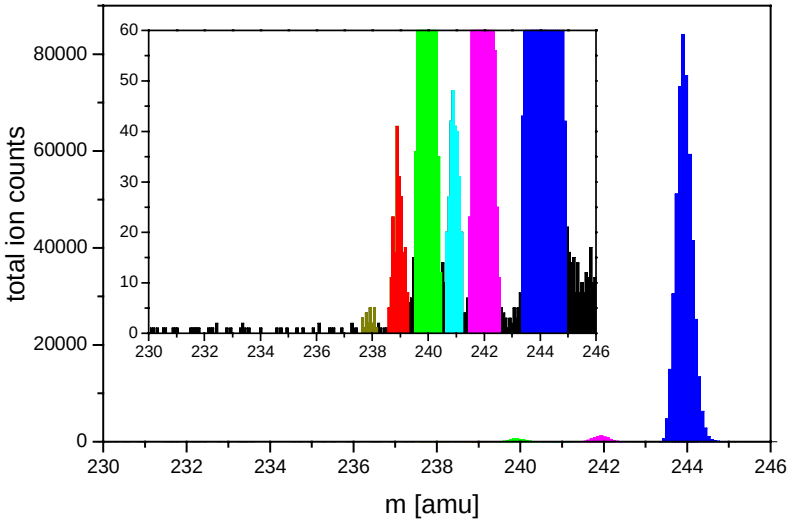

Fig. 8. Mass spectrum of the NIST standard SRM996 with of ∼10^{12} atoms of ^{244}Pu showing all plutonium isotopes present in the sample. The insert is an enlargement of the whole spectrum by a factor of 1500.

Table 3
Measured and certified values for isotope ratios of the SRM996 standard relative to ^{244}Pu

	Isotopes				
	^{238}Pu	^{239}Pu	^{240}Pu	^{241}Pu	^{242}Pu
Measured	0.00004(3)	0.00039(9)	0.0065(4)	0.00054(10)	0.0137(5)
Certified	0.00004(1)	0.00035(2)	0.0069(1)	0.00037(2)	0.0135(1)

Errors are given with 3σ confidence level.

Table 4
Isotope ratio measurements of a stock solution containing ^{239}Pu, ^{240}Pu, and ^{244}Pu

Ratios	Calculated	Measured values				
		1	2	3	4	5
^{239}Pu/^{244}Pu	0.55	0.51(6)	0.55(4)	0.55(4)	0.54(1)	0.57(2)
^{240}Pu/^{244}Pu	0.18	0.19(1)	0.19(1)	0.18(1)	0.16(2)	0.18(1)

Errors are given with 3σ confidence level.

in environmental samples, ^{239}Pu and ^{240}Pu. The results of five measurements are shown in Table 4. There is a very good agreement between measured and calculated values according to the known amounts of ^{239}Pu, ^{240}Pu, and ^{244}Pu in the cocktail.

7. Conclusions

A new Nd:YAG pumped titanium–sapphire laser system has been set up, characterized, and applied for spectroscopic investigations. An efficient three step excitation and ionization scheme for plutonium has been found (with $\lambda_1 = 420.76$ nm, $\lambda_2 = 847.28$ nm, and $\lambda_3 = 767.53$ nm) and the isotope shifts for the long-lived plutonium isotopes from 239 to 242 and 244 have been measured together with the saturation behavior for all three excitation steps. The efficiency of the RIMS system with a TOF mass spectrometer for the detection of a single plutonium isotope has been determined to $\varepsilon_{\mathrm{RIMS}} = 1 \times 10^{-5}$ resulting in a detection limit of 2×10^6 atoms of plutonium for single isotope measurements. It could be demonstrated that isotope ratios can be measured correctly and reproducibly over up to four orders of magnitude. This shows that the new RIMS setup is well-suited for the isotope selective ultratrace analysis of plutonium, e.g., in environmental samples.

References

[1] W.C. Hanson (Ed.), Transuranic Elements in the Environment, Technical Information Center/U.S. Department of Energy, DOE/TIC-22800, 1980.
[2] P.J. Kershaw, D.C. Denoon, D.S. Woodhead, J. Environ. Radioact. 44 (1999) 191.
[3] P. Peuser, H. Gabelmann, M. Lerch, B. Sohnius, N. Trautmann, M. Weber, G. Herrmann, H.O. Denschlag, W. Ruster, J. Bonn, IAEA-SM 252 (40) (1981) 257.
[4] M.H. Dai, K.O. Buesseler, J.M. Kelley, J.E. Andrews, S. Pike, J.F. Wacker, Radioactivity 53 (2001) 9.
[5] S.H. Lee, J. Gastaud, J.J. La Rosa, L. Liong Wee Kwong, P.P. Povinec, E. Wyse, L.K. Fifield, P.A. Hausladen, L.M. Di Tada, G.M. Santos, J. Radioanal. Nucl. Chem. 248 (2001) 757.
[6] J.S. Becker, H.-J. Dietze, in: R.A. Meyers (Ed.), Encyclopedia of Analytical Chemistry, Wiley, New York, 2002, p. 1294.
[7] J.S. Becker, H.-J. Dietze, J. Anal. At. Spectrom. 14 (1999) 1493.
[8] G. Huber, G. Passler, K. Wendt, J.V. Kratz, N. Trautmann, in: M.F. L'Annunziata (Ed.), Handbook of Radioactivity Analysis, Academic Press, San Diego, 2003, p. 799.
[9] J.S. Becker, Spectrochim. Acta B 58 (2003) 1757.
[10] S.F. Boulyga, D. Desideri, M.A. Meli, C. Testa, J.S. Becker, Int. J. Mass Spectrom. 226 (2003) 329.
[11] M.E. Ketterer, K.M. Hafer, C.L. Link, D. Kolwaite, J. Wilson, J.W. Mietelski, J. Anal. At. Spectrom. 19 (2004) 241.
[12] M.V. Zoriy, C. Pickhardt, P. Ostapczuk, R. Hille, J.S. Becker, Int. J. Mass Spectrom. 232 (2004) 217.
[13] C. Tuniz, J.R. Bird, D. Fink, G.F. Herzog (Eds.), Accelerator Mass Spectrometry, CRC Press LLC, Boca Raton, 1998.
[14] L.K. Fifield, Rep. Prog. Phys. 62 (1999) 1223.
[15] L.K. Fifield, Nucl. Instrum. Methods Phys. Res. 172B (2000) 134.
[16] G.S. Hurst, M.H. Nayfey, J.P. Young, Phys. Rev. A 15 (1977) 2283.
[17] D.L. Donohue, J.P. Young, Anal. Chem. 55 (1983) 378.
[18] K. Wendt, N. Trautmann, B.A. Bushaw, Nucl. Instrum. Methods Phys. Res. B 172 (2000) 162.
[19] W. Ruster, F. Ames, H.-J. Kluge, E.W. Otten, D. Rehklau, F. Scheerer, G. Herrmann, C. Mühleck, J. Riegel, H. Rimke, P. Sattelberger, N. Trautmann, Nucl. Instrum. Methods A 281 (1989) 547.
[20] G. Passler, N. Erdmann, H.-U. Hasse, G. Herrmann, G. Huber, S. Köhler, J.V. Kratz, A. Mansel, M. Nunnemann, N. Trautmann, A. Waldek, Kerntechnik 62 (1997) 85.
[21] M. Nunnemann, N. Erdmann, H.-U. Hasse, G. Huber, J.V. Kratz, P. Kunz, A. Mansel, G. Passler, O. Stetzer, N. Trautmann, A. Waldek, J. Alloys Compd. 271–273 (1998) 45.
[22] S. Köhler, R. Deißenberger, K. Eberhardt, N. Erdmann, G. Herrmann, G. Huber, J.V. Kratz, M. Nunnemann, G. Passler, P.M. Rao, J. Riegel, N. Trautmann, K. Wendt, Spectrochim. Acta B 52 (1997) 717.
[23] N. Erdmann, M. Nunnemann, K. Eberhardt, G. Herrmann, G. Huber, S. Köhler, J.V. Kratz, G. Passler, J.R. Peterson, N. Trautmann, A. Waldek, J. Alloys Compd. 271–273 (1998) 837.
[24] K. Wendt, K. Blaum, B.A. Bushaw, C. Grüning, R. Horn, G. Huber, J.V. Kratz, P. Kunz, P. Müller, W. Nörtershäuser, M. Nunnemann, G. Passler, A. Schmitt, N. Trautmann, A. Waldek, Fresenius J. Anal. Chem. 364 (1999) 471.
[25] E.F. Worden, L.R. Carlson, S.A. Johnson, J.A. Paisner, R.W. Solarz, J. Opt. Soc. Am. B10 (1993) 1998.
[26] B. Eichler, S. Hübener, N. Erdmann, K. Eberhardt, H. Funk, G. Herrmann, S. Köhler, N. Trautmann, G. Passler, F.-J. Urban, Radiochim. Acta 79 (1997) 221.
[27] F.-J. Urban, R. Deißenberger, G. Herrmann, S. Köhler, J. Riegel, N. Trautmann, H. Wendeler, F. Albus, F. Ames, H.-J. Kluge, S. Kraß, F. Scheerer, Inst. Phys. Conf. Ser. 128 (1992) 233.
[28] W. Rapoport, C.P. Khattak, Appl. Opt. 27 (1988) 2677.
[29] W. Koechner, Solid State Laser Engineering, Springer, Berlin, 1996.
[30] R. Horn, C. Rauth, J.V. Kratz, K. Wendt, in preparation.
[31] C. Grüning, N. Erdmann, G. Huber, P. Klopp, J.V. Kratz, P. Kunz, M. Nunnemann, G. Passler, A. Waldek, K. Wendt, Reson. Ionization Spectrosc. AIP Conf. Proc. 454 (1998) 285.
[32] J. Blaise, J.-F. Wyart, Selected Constants, Tables Internationales de Constantes, vol. 20, Universite P. et M. Curie, Paris, 1992.
[33] W.M. Fairbanks Jr., M.T. Spaar, J.E. Parks, J.M.R. Hutchinson, Phys. Rev. A40 (1989) 2195.
[34] P. Lambropoulos, A. Lyras, Phys. Rev. A40 (1989) 2199.